

ImagiNet: A Multi-Content Dataset for Generalizable Synthetic Image Detection via Contrastive Learning

Delyan Boychev^{1,2} and Radostin Cholakov^{3,4}

¹ High School of Natural Sciences and Mathematics Veliko Tarnovo, Bulgaria

² Sofia University

delyan.boychev05@gmail.com

³ High School of Mathematics Plovdiv, Bulgaria

⁴ Stanford University

radicho@stanford.edu

Abstract. Generative models, such as diffusion models (DMs), variational autoencoders (VAEs), and generative adversarial networks (GANs), produce images with a level of authenticity that makes them nearly indistinguishable from real photos and artwork. While this capability is beneficial for many industries, the difficulty of identifying synthetic images leaves online media platforms vulnerable to impersonation and misinformation attempts. To support the development of defensive methods, we introduce ImagiNet, a high-resolution and balanced dataset for synthetic image detection, designed to mitigate potential biases in existing resources. It contains 200K examples, spanning four content categories: photos, paintings, faces, and uncategorized. Synthetic images are produced with open-source and proprietary generators, whereas real counterparts of the same content type are collected from public datasets. The structure of ImagiNet allows for a two-track evaluation system: i) classification as real or synthetic and ii) identification of the generative model. To establish a baseline, we train a ResNet-50 model using a self-supervised contrastive objective (SelfCon) for each track. The model demonstrates state-of-the-art performance and high inference speed across established benchmarks, achieving an AUC of up to 0.99 and balanced accuracy ranging from 86% to 95%, even under social network conditions that involve compression and resizing. Our data and code are available at <https://github.com/delyan-boychev/imaginet>.

Keywords: Synthetic Image Detection · Contrastive Learning

1 Introduction

State-of-the-art generative models are rapidly improving their ability to produce nearly identical images to authentic photos and artwork. Diffusion models (DMs) [19,41], variational auto-encoders (VAEs) [17], and generative adversarial

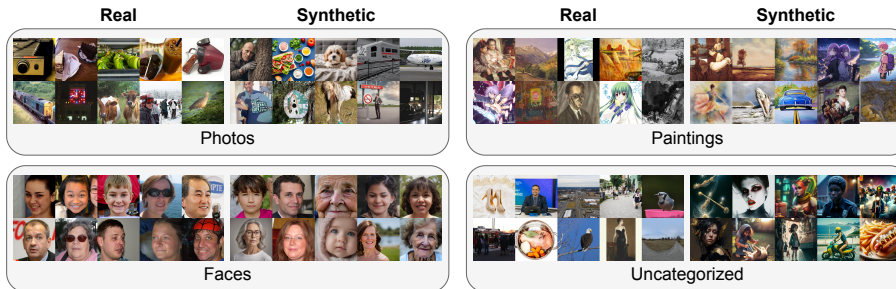


Fig. 1: Examples from each category of the ImagiNet dataset.

networks (GANs) [15] are being utilized in various ways to achieve data augmentation, text-to-image and image-to-image generation, inpainting and outpainting. They facilitate the production of visuals and spatial effects for downstream use in the entertainment, gaming, and marketing industries. On the other hand, these models can be misused by malicious actors. For instance, deceiving content and fake news [32] can be easily generated. Also, the flood of synthetic images and videos overwhelms moderation in content delivery platforms and social networks. Such issues are typically challenging and time-consuming to be solved manually. Thus, there is an increasing demand for improved synthetic image recognition models. Previous research [12, 16, 52] utilizes standard classifier training approaches to produce models with adequate performance on the task. They [12, 16] rely on a dataset with a single source of synthetic examples and a no-downsampling architecture to improve the performance of the detectors on images from unseen generators. These approaches do not completely solve the highly complex task of synthetic content detection due to overfitting, unreliability to detect novel generators, or biases toward various content types. Thus, important aspects of synthetic detection that have yet to be fully explored are the curation of a training dataset with a more diverse selection of content types and the utilization of training techniques better suited for generalizable detectors.

We propose a new benchmark and balanced training set for synthetic image detection called ImagiNet (Figure 1). It includes images from state-of-the-art open-source and proprietary generators. Our main goal is to solve the problem with generalizability by training on diverse data. The images are created by either GAN [15], DM [40], or a proprietary generator – Midjourney [20] or DALL·E [6]. Our benchmark has two main testing tracks – synthetic image detection and model identification. The testing is conducted under perturbations such as JPEG compression and resizing, simulating social network conditions similarly to previous works [12]. For more consistent results, all the images are high-resolution, like the ones posted on social networks.

As discussed in other works, contrastive learning methods for pre-training detectors can achieve state-of-the-art performance on synthetic content detection. Wu *et al.* [52] utilize the textual embedder CLIP [38] to contrast image represen-

tations and class descriptions (e.g. "real photo", "synthetic painting") embeddings. However, it makes the training procedure computationally expensive and rather slow. Instead, we provide a more efficient contrastive baseline model for our dataset. The training paradigm we examine is called Self-Contrastive Learning (SelfCon) [4]. It is a modification of the Supervised Contrastive Learning method [25], which requires a multi-viewed (twice augmented) batch to improve the performance by allowing contrast of a single image within a batch. Self-Con provides a multi-exit architecture consisting of a standard network and a sub-network that can be attached to the intermediate layers. Its function is to produce variations of the embeddings in the latent space, acting as data augmentation. The training procedure has two stages: backbone pre-training and classifier training. The approach is suited to the structure of our dataset and allows for solving multiple tasks during training - real or synthetic classification and model identification.

2 Related Work

2.1 Previous Synthetic Datasets

Previous training and evaluation datasets (Table 1) present a large number of images for training and testing. Many of them include primarily images generated by GANs. However, contemporary generation approaches, such as DMs, often provide advantages in resolution and quality [13] compared to GANs. Thus, training on datasets limited to low-resolution images or primarily focusing on a specific set of generators [12, 16], often excluding proprietary models [52], can lead to limitations in the performance when detecting images from other unseen generators. Another significant problem is the lack of multiple content types during the training procedure, which makes the models potentially prone to overfitting. All these structural problems contribute to the introduction of biases [50].

Rahman *et al.* [39] propose a great alternative for benchmarking synthetic image detectors because of the high number of generators included and the diverse content types. However, neither a training set nor baseline weights are provided for comparison and benchmarking, limiting the dataset only for evaluation. Additionally, the dataset's low-resolution images and the lack of balance may further constrain its application in the area.

2.2 Contrastive Learning

Contrastive Learning [11] is a training paradigm that produces generalizable models and is able to solve multiple representation learning tasks with one training objective – characteristics we find useful in synthetic image detection [53]. Optimizing contrastive objective clusters the representation vectors of training examples in the latent space.

The objective can be self-supervised, semi-supervised, or supervised and is inspired by N-pair losses [47]. In the self-supervised approach [9], an augmented

Table 1: Feature comparison of previous synthetic datasets.. "-" signifies that data is not available. The maximum resolutions are mentioned below.

Training/Benchmark	Corvi2022 [12]	Wu2023 [52]	ArtiFact [39]	Ours
Balanced	✓/ ✗	✓/ ✓	- / ✗	✓/ ✓
Multiple generators	✗/ ✓	✓/ ✓	- / ✓	✓/ ✓
Proprietary generators	✗/ ✓	✗/ ✓	- / ✗	✓/ ✓
Multiple content types	✗/ ✗	✓/ ✓	- / ✓	✓/ ✓
Synthetic images resolution	256 × 256 / 1024 × 1024	1024 × 1024 / 8000 × 8000	- / 200 × 200	1792 × 1024 / 1792 × 1024

copy of an input produces a representation (positive example) to be pulled closer to the anchor (original input) representation. The remaining images and their augmentations (negative examples) are pushed away in the latent space. In the semi-supervised and supervised approaches, images labelled as a given class and their augmented versions are included in the positive examples.

The contrastive learning involves pre-training a backbone encoder $F(\cdot)$, e.g. ResNet-50 [18], which consists of feature-extraction convolutional layers. The encoder is attached to a Multilayer Perceptron [34] with Rectified Linear Unit (ReLU) [26] activation. This part of the architecture is referred to as a *projection head* $H(\cdot)$, which outputs the normalized embeddings in l_2 space. It has been shown that without this component, the performance of the network degrades significantly [9].

For each batch, we sample N examples and augment them twice to get $2N$ inputs $A \equiv \{1, \dots, 2N\}$. We denote the first image of each pair as x_i – anchor – and the second one as $x_{j(i)}$ – positive example. The anchor is contrasted with the other $2(N - 1)$ data points. The output of the network for a given input image is $\omega(x) = H(F(x))$. Therefore the contrastive loss for all positive pairs is as follows:

$$\mathcal{L}_{SelfSup} = - \sum_{i \in A} \log \frac{\exp(\omega(x_i) \cdot \omega(x_{j(i)})) / \tau}{\sum_{l \in Q(i)} \exp(\omega(x_i) \cdot \omega(x_l)) / \tau} \quad (1)$$

where $Q(i) \equiv A \setminus \{i\}$ (similarity between z_i and z_i is redundant), and τ is a temperature parameter. The dot product yields the cosine similarity between the vectors, as they are normalized in l_2 space.

Supervised Contrastive Learning However, the self-supervised loss is impractical when we have labels \hat{y} for all images in the batch. The Supervised Contrastive Loss (SupCon) [25] allows us to pull together all positive examples $P(i) \equiv \{p \in Q(i) : \hat{y}_p = \hat{y}_i\}$ for a given anchor x_i and push the rest of the negatives. With these terms added, we achieve the Supervised Contrastive loss:

$$\mathcal{L}_{SupCon} = \sum_{i \in A} \frac{-1}{|P(i)|} \sum_{p \in P(i)} \log \frac{\exp(\omega(x_i) \cdot \omega(x_p)/\tau)}{\sum_{l \in Q(i)} \exp(\omega(x_i) \cdot \omega(x_l)/\tau)}, \quad (2)$$

where we compute the loss for each example as an anchor and the average for each positive example of the given anchor.

Self-Contrastive Supervised Learning Self-Contrastive Learning [4] offers a twice faster alternative to SupCon. A sub-network is attached to the backbone. Its main responsibility is to produce an alternative view of the images in the latent space instead of additional augmented samples to design the SelfCon loss with a single-viewed batch (augmented once). The sub-network could be a fully connected layer or another architecture with the same function as the backbone. The sub-net $H_{sub}(\cdot)$ is attached to the backbone and projects the latent representations $F_m(\cdot)$ obtained after the m -th ResNet block. The network has two output mapping functions $\Omega \equiv \{H_{sub}(F_m(\cdot)), H(F(\cdot))\}$ for a given input x_i . By introducing this set, we achieve each vector pair (from the main network and the sub-network) for a given input but with $A \equiv \{1, \dots, N\}$ because this method requires only a single augmentation:

$$\mathcal{L}_{SelfCon} = \sum_{\substack{i \in A, \\ \omega \in \Omega}} \frac{-1}{|P(i)||\Omega|} \sum_{\substack{p \in P(i), \\ \omega' \in \Omega}} \log \frac{\exp(\omega(x_i) \cdot \omega'(x_p)/\tau)}{\sum_{l \in Q(i)} \exp(\omega(x_i) \cdot \omega'(x_l)/\tau)} \quad (3)$$

After the pre-training, a calibration stage is performed. A classifier is fitted to the representations generated by the pre-trained backbone encoder. The encoder’s weights remain frozen during this stage, allowing the classifier to adapt to the established latent distribution.

3 Methods

3.1 Dataset Construction

The ImagiNet dataset consists of images from various open-source and proprietary image generators to encompass the distinct "fingerprints" they impart. Dataset’s name combines *imagine*, an often-used instruction in text-to-image generation, with the status quo naming of visual databases used in computer vision. *Imagination* also emphasizes that we focus on the content type diversity of the images generated through creative prompts.

Dataset Structure (Table 2) – The dataset structure is designed to represent real-world scenarios where images of different content types might be used. ImagiNet examples are split into two main categories – real and synthetic images. To mitigate content-related biases, the dataset is divided into four subcategories—photos, paintings, faces, and uncategorized. Such images are commonly found on the World Wide Web and are the main subject of generative applications. We provide a balanced amount of synthetically generated images and

Table 2: ImagiNet dataset structure with two main categories and four subcategories. * signifies images sourced from public datasets.

Real		Synthetic	
Source	Number	Source	Number
Photos (30%)			
ImageNet [43]	7.5K	StyleGAN-XL [44]	7.5K
LSUN [54]	7.5K	ProGAN* [21]	7.5K
COCO [27]	15K	SD v2.1 [40]/SDXL v1.0 [37]	15K
Paintings (22.5%)			
WikiArt [48]	11.25K	StyleGAN3 [23]	11.25K
		SD v2.1 [40]/SDXL v1.0 [37]	5.625K
Danbooru [3]	11.25K	AniImagine XL [49]	5.625K
Faces (22.5%)			
FFHQ [24]	22.5K	StyleGAN-XL [44]	11.25K
		SD v2.1 [40]/SDXL v1.0 [37]	11.25K
Uncategorized (25%)			
Photozilla [46]	25K	Midjourney* [20]	12.5K
		DALL·E 3* [6]	12.5K
Total	100K	Total	100K

real counterparts in each subcategory. The source datasets and generator models are given in Table 2. Images from models marked with * are sourced as follows: ProGAN from Wang *et al.* [51], Midjourney from Pan *et al.* [35], DALL·E 3 from LAION [2]; in addition we generated 800 DALL·E 3 images to reach our desired dataset size by prompting it through the OpenAI API. The unmarked synthetic groups are generated automatically using the respective pre-trained models. Samples from all GAN models are labelled with the GAN category, and samples from the Stable Diffusion variants are labelled as diffusion for the model detection task. Proprietary models are labelled as standalone categories. A detailed analysis of the presence of multiple content types and synthetic generators is available in the supplementary materials.

Real Images Sampling – The real images are randomly sampled from each real counterpart dataset placed in Table 2. The images in our test set are sampled from the validation and testing parts of these sets.

Image Generation Procedure – To generate images with GANs, we sample random latent code (it is selected according to model requirements) for a given seed and feed the generator with it unconditionally. For DMs and private generators (SD v2.1, SDXL v1.0, AniImagine XL, DALL·E 3), however, textual guidance is needed, thus we first search manually for appropriate negative prompts and positive suffixes to increase the quality of the produced images. The construction of each prompt is in descriptive form. For photos, we utilize the captions from COCO [10] to prompt the generators and achieve images with sufficient quality. For paintings, instead of using a pre-generated set of captions for prompting, we create lists of styles, techniques, and subjects with GPT-3.5 Turbo [7]. After that, we fit these characteristics of the paintings in a descriptive sentence shown in Figure 2a, which guides the model to generate varied images. The gaps are filled respectively with an item from the given list, and in the

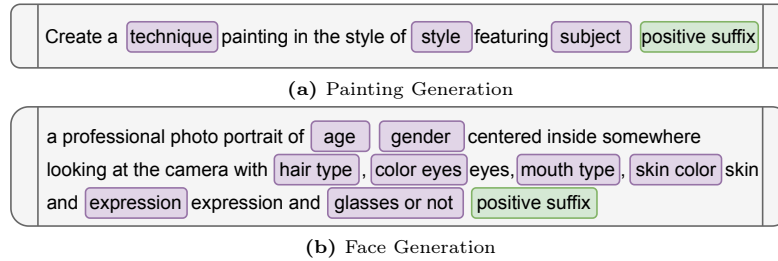


Fig. 2: Prompt structures for image generation.

end, a positive suffix is added. The procedure for face generation is similar – Figure 2b presents the structure of the prompt. All the lists for filling in the guiding instructions, as well as the positive suffixes and negative prompts, are available in our supplementary material. The last model AnimateXL, a fine-tuned SDXL [37] variant for art generation, uses only tags from the Danbooru dataset [3] for prompting.

Dataset Splits – From the whole set, we sample 80% of the images from each category and subcategory with an equal number of images from the different generators. The number of images in the training set is 160K, respectively 40K are left for testing. Because of the contrastive approach that we apply, we need a balanced calibration set sampled from the training set (an equal number of images for each model). It consists of 80K examples in total.

Labellings and Evaluation Tracks – All the images of the dataset are labelled. They have four labels – source (real or synthetic), content type, generator group (GAN, SD, etc.), and specific generator. In our benchmark, we have two tracks – synthetic image detection and model identification. On the test set are applied perturbations to simulate social network conditions [12]. First, we do a large square crop (ranging from 256 to the smaller dimension of the image) of the image and, after that, resize it to 256×256 . After that, we compress 75% of the images with JPEG or WebP compression.

Dataset Access – We provide the synthetic images we generated for this work, along with those from DALL-E 3, which are collected under a Creative Commons Zero license. Both the real counterparts and the additional part of synthetic content (Midjourney and ProGAN examples) can be downloaded from their sources. The whole dataset can be reconstructed with the scripts in our repository, which also includes the list of sources and our synthetic data.

3.2 Training Procedure

To train our model, we first initialize the ResNet-50 model with pre-trained ImagiNet weights and modify its early layers to avoid downsampling, following Gragnaniello *et al.* [16]. In the first stage, we train the backbone with a compound contrastive objective $\mathcal{L}_{SelfCon}$. In our case, the mapping functions $H(\cdot)$ and $H_{sub}(\cdot)$ output representations in \mathbb{R}^{128} . This involves accumulating $\mathcal{L}_{SelfCon}$

applied on two labellings - synthetic detection and model identification labels, with each loss assigned equal weight. When optimizing the model detection objective, real images in the batch are ignored. To address the increased memory demands of removing downsampling in early ResNet-50 layers and the large batch size requirements of SelfCon, we adopt gradient caching [14], a technique initially designed for language model contrastive losses. We modify⁵ it for use with SelfCon [4], SupCon [25], and SimCLR [9]. This approach calculates the loss on the entire batch but accumulates gradients in smaller chunks, allowing for large batch sizes and efficient training on memory-constrained GPUs.

The second stage involves calibrating the model. We detach the sub-network and projection heads, replacing the output projection head with a multilayer perceptron classifier. This classifier is then trained using cross-entropy loss on a balanced dataset to perform both origin and model detection. We update the batch normalization statistics within the backbone’s residual blocks, following Schneider *et al.* [45], to enhance robustness against perturbations not encountered during pre-training.

4 Experiments and Results

We provide a single model following the procedure explained in Section 3.2. During the first stage, the backbone is optimized with SGD [42] for 400 epochs with batch size $N = 200$ on the ImagiNet training set. The initial learning rate of 0.005 is warmed up linearly [31] for 10 epochs and is cosine annealed [29] afterwards. The second stage continues for 5 epochs with AdamW optimizer [29] and constant learning rate 0.0001, weight decay 0.001, $\beta_1 = 0.9$ and $\beta_2 = 0.99$. After the pre-training procedure, we visualize the model representations of the images in the test set by applying Autoencoder dimensionality reduction [33] (discussed in supplementary materials). We obtain the plots in Figure 3 with our model’s representations computed on center-cropped images from our test set. The plots show the ability of our model to distinguish between real and synthetic images as well as to cluster each generator’s images.

Additionally, we train a model on the ImagiNet training set utilizing the Corvi *et al.* [12] approach and fine-tune the classifier to have a fair comparison with our novel method. This calibration method did not result in a statistically significant improvement in either accuracy or AUC on average across different benchmarks⁶.

4.1 Synthetic Detection Track

Testing Settings – In our evaluation report, we showcase our model and four other approaches - Grag2021 [16] trained on StyleGAN images, Corvi2022 [12]

⁵ Our implementation of gradient caching for contrastive objectives is available at <https://github.com/delyan-boychev/grad-cache-con-learning>

⁶ The fine-tuned classifier is not included in the comparison, as its performance is statistically indistinguishable from the presented model.

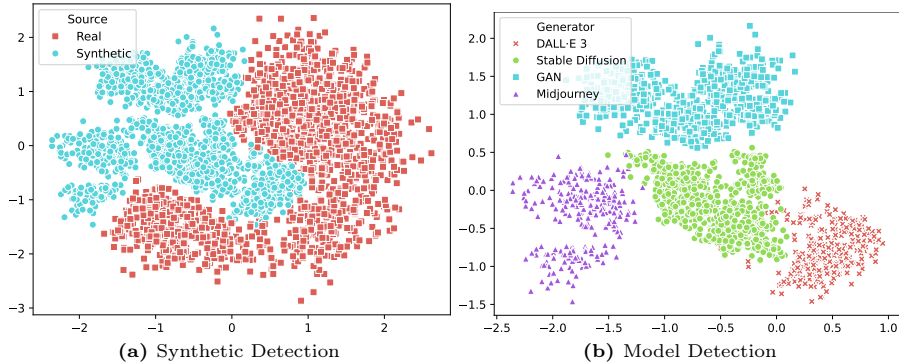


Fig. 3: Dimensionality reduction plots of the representations of the model computed on a part of the ImagiNet test set.

(where logits of two classifiers are fused), Wu2023 [52], and Corvi2022 [12] trained on ImagiNet training set (a single model). The raw probabilities are computed following the requirements of each model. Wu2023 detector leverages cosine similarity for predictions. To accommodate this approach, an anchor vector is required, which is obtained from real images by averaging their latent representations at the final layer of the network. For model-to-model comparability, we derive a distinct anchor vector for each test set, estimated using 100 real images drawn from the corresponding benchmark. Furthermore, the predicted probabilities of the detectors are calibrated with the Platt scaling method [36] by sampling 2 real and 2 synthetic images from each generator in the given test set. For the ImagiNet benchmark, we sample 10 real and 10 synthetic to mitigate potential biases since the GAN and SD categories contain different approaches to generative modeling. We evaluated the performance of all approaches against two established benchmarks: The practical test set (Table 3) and Corvi’s test set (Table 4). We also tested the detectors on our novel benchmark – ImagiNet (Table 5). The practical test is designed to assess detection performance under ideal conditions. It utilizes 448×448 crops extracted from the original image. Corvi’s and ImagiNet benchmarking are conducted with a random large crop, followed by a resize to 256×256 and Jpeg or WebP compression on the images to simulate social network scenarios.

Discussion – On the Practical test set, our model outperforms the Wu2023 approach, yielding almost 7% improvement in ACC and 4% in AUC on average. Importantly, our approach exhibits strong generalization capabilities, performing effectively on unseen generators (DreamBooth, NightCafe, and YiJian) even without explicit training data from them and outperforming Wu2023 on two of them while preserving the same results on the third. The Grag2021 method, trained only on StyleGAN images, underperforms on YiJian (community model, part of NightCafe [1]). It achieves lower accuracy than 50%, suggesting the detector’s inability to generalize over the different generators’ examples, giving predictions similar to a random classifier. The Corvi2022 approach almost matches

Table 3: Results on Practical test set [52] in terms of accuracy and AUC. Detectors marked with * are trained on the ImagiNet dataset. **Bold/Underline** indicates best ACC/AUC.

ACC / AUC	Grag2021	Corvi2022	Wu2023	Corvi2022*	Ours*
DreamBooth	0.5295 / 0.5737	0.8574 / 0.9456	0.9049 / 0.9733	0.9572 / 0.9928	0.9601 / <u>0.9950</u>
MidjourneyV4	0.6521 / 0.7267	0.8316 / 0.9206	0.8907 / 0.9495	0.9542 / 0.9930	0.9675 / <u>0.9959</u>
MidjourneyV5	0.5200 / 0.5322	0.7580 / 0.8389	0.8540 / 0.9224	0.9655 / 0.9975	0.9745 / <u>0.9991</u>
NightCafe	0.6531 / 0.7045	0.6654 / 0.7248	0.8962 / <u>0.9652</u>	0.8654 / 0.9324	0.8931 / 0.9644
StableAI	0.6256 / 0.6744	0.8713 / 0.9500	0.8806 / 0.9534	0.9527 / 0.9885	0.9574 / <u>0.9947</u>
YiJian	0.4271 / 0.4232	0.7224 / 0.8317	0.8392 / 0.9233	0.8266 / 0.9174	0.9045 / <u>0.9726</u>
Mean	0.5679 / 0.6058	0.7843 / 0.8686	0.8776 / 0.9479	0.9203 / 0.9703	0.9428 / <u>0.9870</u>

Table 4: Results on Corvi’s test set [12] in terms of accuracy and AUC. Detectors marked with * are trained on the ImagiNet dataset. **Bold/Underline** indicates best ACC/AUC.

ACC / AUC	Grag2021	Corvi2022	Wu2023	Corvi2022*	Ours*
ProGAN	0.8246 / <u>0.9998</u>	0.9117 / 0.9994	0.9230 / 0.9992	0.9030 / 0.9995	0.8974 / 0.9991
StyleGAN2	0.8236 / <u>0.9805</u>	0.8662 / 0.9455	0.7525 / 0.8495	0.8675 / 0.9479	0.8884 / 0.9759
StyleGAN3	0.8226 / <u>0.9644</u>	0.8557 / 0.9416	0.7395 / 0.8468	0.8705 / 0.9440	0.8824 / <u>0.9707</u>
BigGAN	0.8236 / <u>0.9938</u>	0.8952 / 0.9699	0.8790 / 0.9507	0.8980 / 0.9882	0.8934 / 0.9864
EG3D	0.8241 / 0.9847	0.9062 / 0.9756	0.7980 / 0.8910	0.8450 / 0.9160	0.8964 / <u>0.9913</u>
Taming Tran	0.8218 / 0.9623	0.9112 / <u>0.9902</u>	0.7775 / 0.8705	0.8538 / 0.9278	0.8829 / 0.9651
DALL-E Mini	0.8201 / 0.9614	0.9117 / <u>0.9914</u>	0.7960 / 0.8806	0.9015 / 0.9792	0.8924 / 0.9786
DALL-E 2	0.5851 / 0.6235	0.6507 / 0.7590	0.5115 / 0.5323	0.7370 / 0.8302	0.7729 / <u>0.8590</u>
GLIDE	0.7856 / 0.8747	0.9062 / <u>0.9780</u>	0.6315 / 0.7052	0.8730 / 0.9429	0.8539 / 0.9347
Latent Diff	0.8048 / 0.9195	0.9117 / <u>0.9998</u>	0.8130 / 0.8959	0.9017 / 0.9989	0.8959 / 0.9902
Stable Diff	0.7461 / 0.8115	0.9117 / <u>0.9999</u>	0.8985 / 0.9710	0.9030 / 0.9998	0.8969 / 0.9956
ADM	0.7331 / 0.8167	0.7927 / <u>0.8772</u>	0.5933 / 0.6716	0.7875 / 0.8710	0.7704 / 0.8550
Mean	0.7846 / 0.9077	0.8692 / <u>0.9523</u>	0.7594 / 0.8387	0.8618 / 0.9446	0.8686 / <u>0.9585</u>

the performance of Wu2023 on Stable Diffusion examples. The other Corvi2022 model trained on the ImagiNet training set has a great improvement in the result compared to previous state-of-the-art detectors, signifying the quality of the dataset and the importance of data diversity. However, this detector has limited generalization abilities to some of the unseen generators (NightCafe, YiJian) when compared to our baseline.

Our baseline performance remains consistent on Corvi’s benchmark as there is no statistically significant difference to the Corvi2022 model – mean ACC almost 87% and mean AUC at 0.95. It shows a substantial improvement of 12% in ACC on DALL-E 2 examples since it is trained on DALL-E 3 images. The results on StyleGAN3 and StyleGAN2 are increased by 1-2%. In comparison to our model, Grag2021 has a higher AUC on almost all GAN sections of the benchmark as it is trained only on GAN examples. However, its performance decreases significantly on all other generators. The Corvi2022 model trained on ImagiNet performs almost the same as our baseline and Corvi2022 detector.

On the ImagiNet benchmark, the SelfCon approach achieves the highest average ACC and AUC across all detectors. It is important to highlight that while

Table 5: Results on ImagiNet synthetic detection track in terms of accuracy and AUC. Detectors marked with * are trained on the ImagiNet dataset. **Bold/Underline** indicates best ACC/AUC.

ACC / AUC	Grag2021	Corvi2022	Wu2023	Corvi2022*	Ours*
GAN	0.6889 / 0.8403	0.6822 / 0.8033	0.6508 / 0.6971	0.8534 / 0.9416	0.9372 / <u>0.9886</u>
SD	0.5140 / 0.5217	0.6112 / 0.6851	0.6367 / 0.6718	0.8693 / 0.9582	0.9608 / <u>0.9922</u>
Midjourney	0.4958 / 0.5022	0.5826 / 0.6092	0.5326 / 0.5289	0.8880 / 0.9658	0.9652 / <u>0.9949</u>
DALL-E 3	0.4128 / 0.3905	0.5180 / 0.5270	0.5368 / 0.5482	0.8906 / 0.9759	0.9724 / <u>0.9963</u>
Mean	0.5279 / 0.5637	0.5985 / 0.6562	0.5892 / 0.6115	0.8753 / 0.9604	0.9589 / <u>0.9930</u>

Table 6: Models inference time in milliseconds for an image with size 448×448 on a single NVIDIA RTX 4090 GPU.

Grag2021	Corvi2022	Wu2023	Ours
24.30	49.53	16.01	25.10

the Corvi2022 model, trained on our ImagiNet dataset, demonstrates improved performance compared to other models, our training method further enhances this performance and stands out in terms of generalizability. This is evident in the near-random classifier accuracy exhibited by other models on proprietary generative models such as Midjourney and DALL-E 3, highlighting their limited ability to generalize beyond the benchmarks lacking data diversity. Further analysis of performance across different content types and specific generators can be found in the supplementary material.

We recognize the critical importance of inference speed in real-world applications. While our proposed model may not achieve the absolute fastest inference (Table 6), it significantly outperforms the state-of-the-art Corvi2022 model, reducing its inference time by half while maintaining comparable accuracy on its test set and surpassing it on others. It signifies the ability of our baseline to balance performance and efficiency, making it a more practical solution for time-sensitive applications.

4.2 Model Identification Track

Testing Settings – For this evaluation track, we use only the synthetic images with the same applied perturbations from the synthetic track.

Discussion – Interestingly, even aggressive perturbations such as resize and compression do not significantly harm the performance of the model identifier (Table 7). The results confirm that each generator has its unique "fingerprints", which are studied in other works [12]. The model identification track is open for evaluation of other novel detectors. Further analysis of the model robustness under perturbations is placed in the supplementary materials.

Table 7: Results of our detector on ImagiNet model identification track in terms of accuracy. The AUC is 0.9980

GAN	SD	Midjourney	DALL·E 3	Mean
0.9968	0.9683	0.9228	0.9160	0.9510

5 Conclusion

In conclusion, we introduce ImagiNet, a high-resolution balanced dataset designed to address the limitations of previous sets in the field of synthetic image detection. They often lack diverse content types and multiple generators, leading to biased detectors. By involving a wide range of content types and generators, including proprietary models, ImagiNet enables the training of more generalizable and robust detectors. The quality of our ImagiNet dataset is demonstrated by the fact that a model trained on it, even with a previous state-of-the-art method, surpasses current detectors on several benchmarks. In addition, we utilize a self-contrastive learning approach that further enhances the model’s generalizability, achieving state-of-the-art results under challenging social network conditions, such as image resizing and compression. Notably, our model reaches this performance while maintaining fast inference speed, making it a practical solution for real-world applications.

6 Acknowledgements

We would like to thank Sangmin Bae for the advice provided. We also acknowledge the America for Bulgaria and Beautiful Science foundations for partially funding the computational resources used as a part of the Diffground OSS project. The Google ML Developer Programs team supported this work by providing Google Cloud and Colab credits.

References

1. Ai art generator: Nightcafe creator, <https://creator.nightcafe.studio/>
2. Dalle-3 images by laion, accessed on 05/11/2023, <https://huggingface.co/datasets/OpenDatasets/dalle-3-dataset>
3. Anonymous, community, D., Branwen, G.: Danbooru2021: A large-scale crowd-sourced and tagged anime illustration dataset. <https://gwern.net/danbooru2021> (January 2022), <https://gwern.net/danbooru2021>
4. Bae, S., Kim, S., Ko, J., Lee, G., Noh, S., Yun, S.Y.: Self-contrastive learning: Single-viewed supervised contrastive framework using sub-network (2022)
5. Bank, D., Koenigstein, N., Giryes, R.: Autoencoders (2021)
6. Betker, J., Goh, G., Jing, L., Brooks, T., Jianfeng Wang, L.L., Ouyang, L., Zhuang, J., Lee, J., Guo, Y., Manassra, W., Dhariwal, P., Chu, C., Jiao, Y., Ramesh, A.: Improving image generation with better captions (2023), <https://cdn.openai.com/papers/dall-e-3.pdf>
7. Brown, T.B., Mann, B., Ryder, N., Subbiah, M., Kaplan, J., Dhariwal, P., Neelakantan, A., Shyam, P., Sastry, G., Askell, A., Agarwal, S., Herbert-Voss, A., Krueger, G., Henighan, T., Child, R., Ramesh, A., Ziegler, D.M., Wu, J., Winter, C., Hesse, C., Chen, M., Sigler, E., Litwin, M., Gray, S., Chess, B., Clark, J., Berner, C., McCandlish, S., Radford, A., Sutskever, I., Amodei, D.: Language models are few-shot learners (2020)
8. Chen, T.: On the importance of noise scheduling for diffusion models (2023)
9. Chen, T., Kornblith, S., Norouzi, M., Hinton, G.: A simple framework for contrastive learning of visual representations (2020)
10. Chen, X., Fang, H., Lin, T.Y., Vedantam, R., Gupta, S., Dollar, P., Zitnick, C.L.: Microsoft coco captions: Data collection and evaluation server (2015)
11. Chopra, S., Hadsell, R., LeCun, Y.: Learning a similarity metric discriminatively, with application to face verification. In: 2005 IEEE Computer Society Conference on Computer Vision and Pattern Recognition (CVPR'05). vol. 1, pp. 539–546 vol. 1 (2005). <https://doi.org/10.1109/CVPR.2005.202>
12. Corvi, R., Cozzolino, D., Zingarini, G., Poggi, G., Nagano, K., Verdoliva, L.: On the detection of synthetic images generated by diffusion models (2022)
13. Dhariwal, P., Nichol, A.: Diffusion models beat gans on image synthesis (2021)
14. Gao, L., Zhang, Y., Han, J., Callan, J.: Scaling deep contrastive learning batch size under memory limited setup (2021)
15. Goodfellow, I.J., Pouget-Abadie, J., Mirza, M., Xu, B., Warde-Farley, D., Ozair, S., Courville, A., Bengio, Y.: Generative adversarial networks (2014)
16. Gragnaniello, D., Cozzolino, D., Marra, F., Poggi, G., Verdoliva, L.: Are gan generated images easy to detect? a critical analysis of the state-of-the-art (2021)
17. Harvey, W., Naderiparizi, S., Wood, F.: Conditional image generation by conditioning variational auto-encoders (2022)
18. He, K., Zhang, X., Ren, S., Sun, J.: Deep residual learning for image recognition (2015)
19. Ho, J., Jain, A., Abbeel, P.: Denoising diffusion probabilistic models (2020)
20. Holz, D.: Midjourney, <https://www.midjourney.com/>
21. Karras, T., Aila, T., Laine, S., Lehtinen, J.: Progressive growing of gans for improved quality, stability, and variation (2018)
22. Karras, T., Aittala, M., Aila, T., Laine, S.: Elucidating the design space of diffusion-based generative models (2022)

23. Karras, T., Aittala, M., Laine, S., Härkönen, E., Hellsten, J., Lehtinen, J., Aila, T.: Alias-free generative adversarial networks (2021)
24. Karras, T., Laine, S., Aila, T.: A style-based generator architecture for generative adversarial networks (2019)
25. Khosla, P., Teterwak, P., Wang, C., Sarna, A., Tian, Y., Isola, P., Maschinot, A., Liu, C., Krishnan, D.: Supervised contrastive learning (2021)
26. Krizhevsky, A., Sutskever, I., Hinton, G.E.: Imagenet classification with deep convolutional neural networks. In: Proceedings of the 25th International Conference on Neural Information Processing Systems - Volume 1. p. 1097–1105. NIPS’12, Curran Associates Inc., Red Hook, NY, USA (2012)
27. Lin, T.Y., Maire, M., Belongie, S., Bourdev, L., Girshick, R., Hays, J., Perona, P., Ramanan, D., Zitnick, C.L., Dollár, P.: Microsoft coco: Common objects in context (2015)
28. Liu, L., Ren, Y., Lin, Z., Zhao, Z.: Pseudo numerical methods for diffusion models on manifolds (2022)
29. Loshchilov, I., Hutter, F.: Sgdr: Stochastic gradient descent with warm restarts (2017)
30. Lu, C., Zhou, Y., Bao, F., Chen, J., Li, C., Zhu, J.: Dpm-solver: A fast ode solver for diffusion probabilistic model sampling in around 10 steps (2022)
31. Ma, J., Yarats, D.: On the adequacy of untuned warmup for adaptive optimization (2021)
32. Masood, M., Nawaz, M., Malik, K.M., Javed, A., Irtaza, A.: Deepfakes generation and detection: State-of-the-art, open challenges, countermeasures, and way forward (2021)
33. Meng, Q., Catchpoole, D., Skillicom, D., Kennedy, P.J.: Relational autoencoder for feature extraction. In: 2017 International Joint Conference on Neural Networks (IJCNN). IEEE (may 2017). <https://doi.org/10.1109/ijcnn.2017.7965877>
34. Murtagh, F.: Multilayer perceptrons for classification and regression. *Neurocomputing* **2**(5), 183–197 (1991)
35. Pan, J., Sun, K., Ge, Y., Li, H., Duan, H., Wu, X., Zhang, R., Zhou, A., Qin, Z., Wang, Y., Dai, J., Qiao, Y., Li, H.: Journeydb: A benchmark for generative image understanding (2023)
36. Platt, J.: Probabilistic outputs for support vector machines and comparisons to regularized likelihood methods. *Adv. Large Margin Classif.* **10** (06 2000)
37. Podell, D., English, Z., Lacey, K., Blattmann, A., Dockhorn, T., Müller, J., Penna, J., Rombach, R.: Sdxl: Improving latent diffusion models for high-resolution image synthesis (2023)
38. Radford, A., Kim, J.W., Hallacy, C., Ramesh, A., Goh, G., Agarwal, S., Sastry, G., Askell, A., Mishkin, P., Clark, J., Krueger, G., Sutskever, I.: Learning transferable visual models from natural language supervision (2021)
39. Rahman, M.A., Paul, B., Sarker, N.H., Hakim, Z.I.A., Fattah, S.A.: Artifact: A large-scale dataset with artificial and factual images for generalizable and robust synthetic image detection (2023)
40. Rombach, R., Blattmann, A., Lorenz, D., Esser, P., Ommer, B.: High-resolution image synthesis with latent diffusion models. In: Proceedings of the IEEE/CVF Conference on Computer Vision and Pattern Recognition (CVPR). pp. 10684–10695 (June 2022)
41. Rombach, R., Blattmann, A., Lorenz, D., Esser, P., Ommer, B.: High-resolution image synthesis with latent diffusion models (2022)
42. Ruder, S.: An overview of gradient descent optimization algorithms (2017)

43. Russakovsky, O., Deng, J., Su, H., Krause, J., Satheesh, S., Ma, S., Huang, Z., Karpathy, A., Khosla, A., Bernstein, M., Berg, A.C., Fei-Fei, L.: Imagenet large scale visual recognition challenge (2015)
44. Sauer, A., Schwarz, K., Geiger, A.: Stylegan-xl: Scaling stylegan to large diverse datasets (2022)
45. Schneider, S., Rusak, E., Eck, L., Bringmann, O., Brendel, W., Bethge, M.: Improving robustness against common corruptions by covariate shift adaptation (2020)
46. Singhal, T., Liu, J., Blessing, L.T.M., Lim, K.H.: Photozilla: A large-scale photography dataset and visual embedding for 20 photography styles (2021)
47. Sohn, K.: Improved deep metric learning with multi-class n-pair loss objective. In: Lee, D., Sugiyama, M., Luxburg, U., Guyon, I., Garnett, R. (eds.) *Advances in Neural Information Processing Systems*. vol. 29. Curran Associates, Inc. (2016)
48. Tan, W.R., Chan, C.S., Aguirre, H., Tanaka, K.: Improved artgan for conditional synthesis of natural image and artwork. *IEEE Transactions on Image Processing* **28**(1), 394–409 (2019). <https://doi.org/10.1109/TIP.2018.2866698>, <https://doi.org/10.1109/TIP.2018.2866698>
49. Taqwa, F.: Animate xl based on sdxl (2024), <https://huggingface.co/Linaqruf/animate-xl>
50. Torralba, A., Efros, A.A.: Unbiased look at dataset bias. In: *CVPR 2011*. pp. 1521–1528 (2011). <https://doi.org/10.1109/CVPR.2011.5995347>
51. Wang, S.Y., Wang, O., Zhang, R., Owens, A., Efros, A.A.: Cnn-generated images are surprisingly easy to spot...for now. In: *CVPR (2020)*
52. Wu, H., Zhou, J., Zhang, S.: Generalizable synthetic image detection via language-guided contrastive learning (2023)
53. Xu, Y., Raja, K., Pedersen, M.: Supervised contrastive learning for generalizable and explainable deepfakes detection. In: *2022 IEEE/CVF Winter Conference on Applications of Computer Vision Workshops (WACVW)*. pp. 379–389 (2022). <https://doi.org/10.1109/WACVW54805.2022.00044>
54. Yu, F., Seff, A., Zhang, Y., Song, S., Funkhouser, T., Xiao, J.: Lsun: Construction of a large-scale image dataset using deep learning with humans in the loop (2016)

A Assessment of Potential Biases

To investigate the influence of specific content types and synthetic image generators on the synthetic image detector and identify potential biases, we conducted an ablation study inspired by Leave-One-Out Cross-Validation (LOOCV). Separate models were trained, each with one category (content type, generator) excluded from its training data, while maintaining equal training data overall. The isolation of the specific category influence allowed us to identify potential biases through drastic changes in performance when tested on the unseen group of examples.

A.1 Content Type

From the synthetic images in our ImagiNet dataset, we focused on those generated by Stable Diffusion due to its presence in all image subcategories, thus eliminating potential generator-specific biases. We sampled a balanced subset containing 4500 real and 4500 synthetic (Stable Diffusion only) images per subcategory (photos, paintings, faces). For each model, we used a ResNet-18 architecture, training it from scratch for 200 epochs to avoid any biases from pre-trained models. Each model was trained on 18000 images with one category left out. This lets us analyze how each type of content affects the detector's performance by comparing it to a baseline model trained on all categories. For evaluation, we sample 1000 real and 1000 synthetic images for each category.⁷

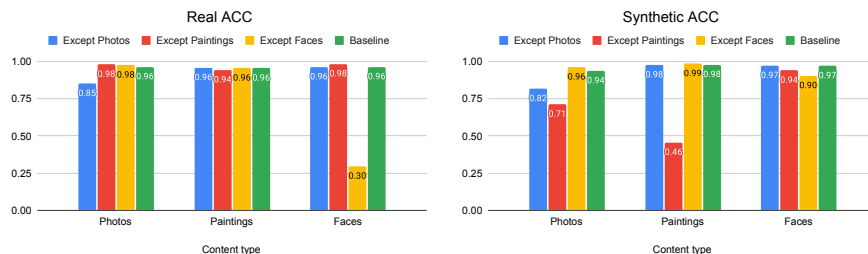


Fig. 4: Real and synthetic accuracy on the different models that are trained by leaving one content type out and the baseline trained on all content types.

The plots presented in Figure 4 and Figure 5 demonstrate that models trained by excluding a specific content type exhibit overfitting and generally lower synthetic accuracy when tested on that content type. Notably, the "Except Faces" model overfits the real image distribution, suggesting that bias is introduced not only by synthetic images but also by real images. The AUC plot in Figure 5

⁷ We investigated a potential bias toward the resolution of real images across different content type groups. However, our analysis revealed no significant bias.

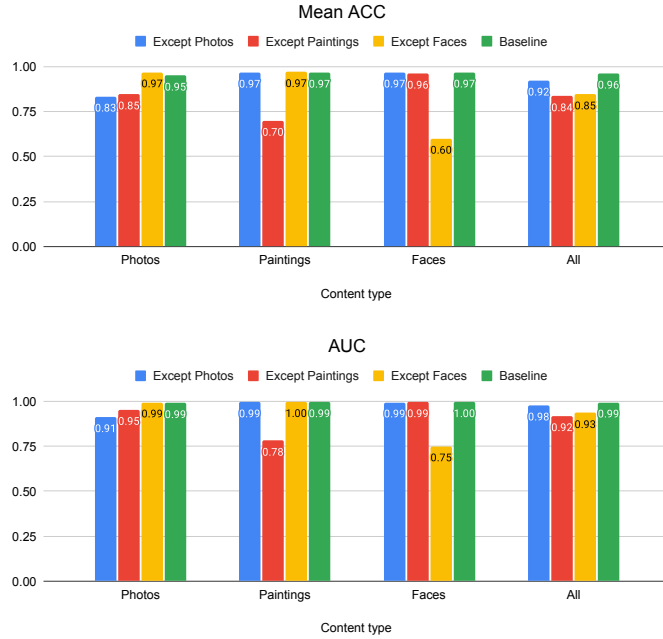


Fig. 5: Mean accuracy and AUC on the different models trained by leaving one content type out and the baseline trained on all content types.

reveals high variance from expected values for the "Except Painting" and "Except Faces" models on their respective content types, highlighting the inability to distinguish between the real and synthetic classes at all possible thresholds. This suggests that training on diverse content types is essential for mitigating bias. The baseline model, trained on all types, does not overfit on the test set and reduces the bias, indicating the suitable setting for these most common content types found on the World Wide Web.

A.2 Synthetic Image Generator

To study biases introduced by different synthetic image generators while excluding biases from varying content types, we focus exclusively on the photos category from our ImagiNet dataset. We sampled a balanced subset containing 4,500 real photographs and 4,500 synthetic photos for each generator (StyleGAN-XL, ProGAN, SD v2.1/SDXL v1.0). We trained three individual ResNet-18 detector models from scratch for 200 epochs, each on 18,000 images, excluding one generator's examples from the training (respectively detectors' names are 'Except StyleGAN-XL', 'Except ProGAN', and 'Except SD'). This allows us to assess the performance of each detector in the absence of influence from a specific generator through the training data, and compare it to a baseline model trained

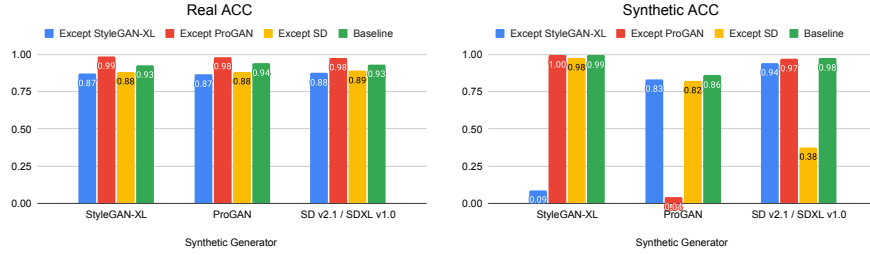


Fig. 6: Real and synthetic accuracy on the different models that are trained by leaving one synthetic generator out and the baseline trained on images from all synthetic generators.

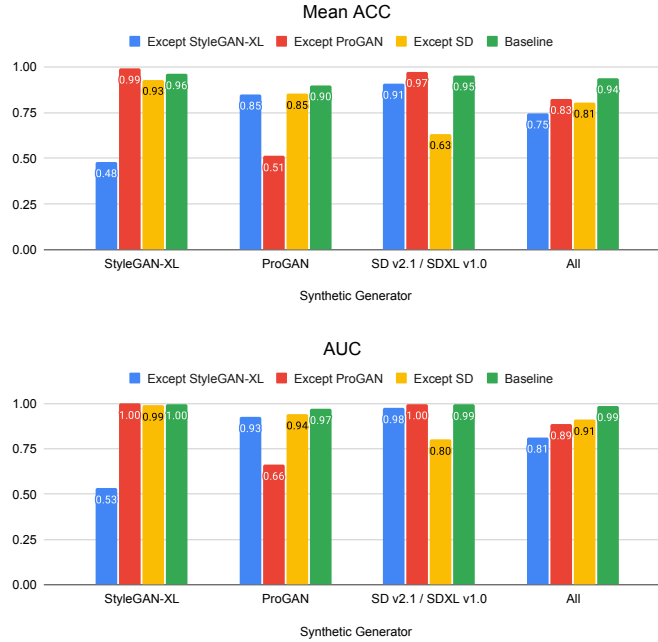


Fig. 7: Mean accuracy and AUC on the different models trained by leaving one synthetic generator out and the baseline trained on examples from all generators.

on all generators. For evaluation, we sampled 1,000 real and 1,000 synthetic images per generator. As shown in the "Real ACC" plot of Figure 6, the diversity of real photos used during training does not significantly affect the accuracy of synthetic image detection, as expected, since we are measuring bias towards synthetic data. In contrast, in the "Synthetic ACC" plot of Figure 6, models tested on images from unseen generators perform poorly, with some barely reaching 0.04% - 0.09% accuracy. This highlights that models struggle to generalize to

Table 8: Results on ImagiNet by content type in terms of accuracy and AUC. Detectors marked with * are trained on the ImagiNet dataset. **Bold/Underline** indicates best ACC/AUC. The range is computed across all content types.

ACC / AUC	Grag2021	Corvi2022	Wu2023	Corvi2022*	Ours*
Photos	0.6676 / 0.7593	0.7203 / 0.8247	0.6933 / 0.7533	0.8820 / 0.9624	0.9643 / <u>0.9933</u>
Paintings	0.5637 / 0.6158	0.6074 / 0.6853	0.5030 / 0.4614	0.7954 / 0.8992	0.9077 / <u>0.9745</u>
Faces	0.5781 / 0.6675	0.5316 / 0.6913	0.6630 / 0.7257	0.8291 / 0.9489	0.9551 / <u>0.9923</u>
Uncategorised	0.4299 / 0.4110	0.6010 / 0.6431	0.5847 / 0.6091	0.9528 / 0.9915	0.9821 / <u>0.9988</u>
Mean	0.5598 / 0.6134	0.6151 / 0.7111	0.6110 / 0.6374	0.8648 / 0.9505	0.9523 / <u>0.9897</u>
Range ↓	0.2371 / 0.3483	0.1884 / 0.1816	0.1900 / 0.2919	0.1566 / 0.0923	0.0743 / <u>0.0243</u>

synthetic images from unseen generators during training. Even models trained on GAN examples, like 'Except StyleGAN-XL' (trained on ProGAN and Stable Diffusion), cannot generalize to images from StyleGAN-XL. The AUC plot in Figure 7 further demonstrates that detectors trained without images from a specific generator fail to distinguish real from the excluded synthetic source, even at various thresholds, indicating the presence of bias related to the synthetic image generator. The performance of the baseline model, trained on diverse synthetic sources, suggests that this diversity enhances the overall detector's generalization.

B Performance of Detectors by Content Type and Specific Generator

Following the procedure outlined in the synthetic track, we conducted an evaluation of detector bias on ImagiNet, focusing on both accuracy and AUC as key performance metrics and grouping the images by content type and specific generator. All detectors included in the comparison are Grag2021 [16], Corvi2022 [12], Wu2023 [52], Corvi2022* [12] trained on our ImagiNet dataset and our SelfCon method. For each content type and specific generator, our model achieved the highest performance in both accuracy and AUC when compared to others (Table 8 and Table 9).

To further investigate potential biases, we examined the range of accuracy and AUC values (difference between maximum and minimum for all categories) across different content types and generators for each model. We chose range as our metric because it clearly shows how much performance varies across different conditions. A smaller range means the model performs more consistently, while a larger range suggests potential biases affecting specific types of content or generators. Our model consistently showed the smallest range in both accuracy and AUC, even compared to Corvi2022 trained on the same data. This indicates that our method is more generalizable and less susceptible to these types of bias.

Table 9: Results on ImagiNet by specific generator in terms of accuracy and AUC. Detectors marked with * are trained on the ImagiNet dataset. **Bold/Underline** indicates best ACC/AUC. The range is computed across all generators.

ACC / AUC	Grag2021	Corvi2022	Wu2023	Corvi2022*	Ours*
ProGAN	0.7250 / 0.9318	0.7350 / 0.9296	0.8127 / 0.9515	0.9050 / 0.9955	0.9767 / <u>0.9986</u>
StyleGAN-XL	0.6731 / 0.8048	0.6477 / 0.7622	0.5824 / 0.6032	0.8775 / 0.9641	0.9603 / <u>0.9942</u>
StyleGAN3	0.6916 / 0.8431	0.7153 / 0.7917	0.6602 / 0.6851	0.7716 / 0.8602	0.8811 / <u>0.9724</u>
SD v2.1	0.5461 / 0.5647	0.6167 / 0.6892	0.6337 / 0.6682	0.8408 / 0.9250	0.9435 / <u>0.9849</u>
SDXL v1.0	0.5645 / 0.5975	0.6240 / 0.7229	0.6112 / 0.6421	0.8968 / 0.9807	0.9767 / <u>0.9987</u>
Animagine XL	0.2853 / 0.1787	0.5218 / 0.5469	0.7289 / 0.7888	0.9098 / 0.9984	0.9778 / <u>0.9996</u>
Midjourney	0.4890 / 0.5016	0.5766 / 0.5996	0.5298 / 0.5240	0.8830 / 0.9634	0.9654 / <u>0.9946</u>
DALL-E 3	0.4204 / 0.3972	0.5254 / 0.5356	0.5336 / 0.5484	0.8894 / 0.9748	0.9700 / <u>0.9964</u>
Mean	0.5494 / 0.6024	0.6203 / 0.6972	0.6366 / 0.6764	0.8717 / 0.9578	0.9564 / <u>0.9924</u>
Range ↓	0.4397 / 0.7531	0.2132 / 0.3940	0.2829 / 0.4275	0.1382 / 0.1382	0.0967 / <u>0.0272</u>

C Model Identification Under Perturbations

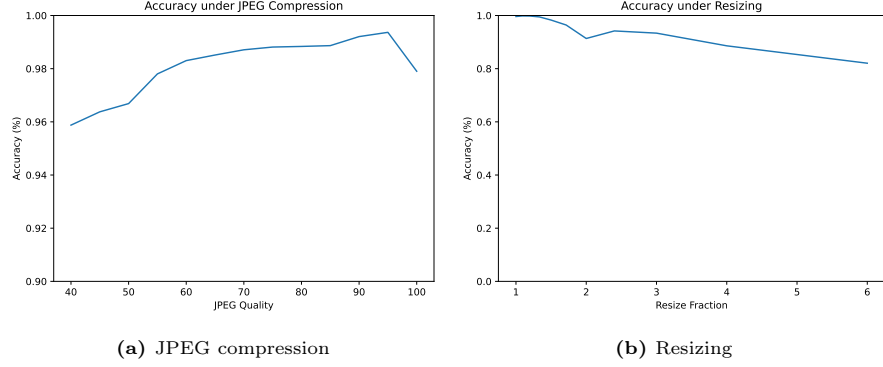
We investigate the robustness of our model’s classification performance under image perturbations, specifically JPEG compression and image resizing with linear scaling of the crop size.

JPEG Compression – The impact of JPEG compression on model performance is presented in Figure 8a. The results indicate that even aggressive JPEG compression with a quality factor as low as 40 does not significantly degrade model performance. This suggests a level of resilience to the artefacts introduced by JPEG compression within our classification model.

Image Resizing – Figure 8b illustrates the model’s performance under image resizing with linear scaling of the crop size. To prepare the images for analysis, we first apply a center crop with dimensions $256r \times 256r$, where r denotes the scaling fraction along the x-axis of the plot. Subsequently, the images are resized to a standard resolution of 256×256 pixels. Similarly, to JPEG compression we have a slight degradation in performance, but with much aggressive perturbation. This suggests that the model is robust to one of the most common augmentations applied to images in social networks.

D Visualizations via Relational Dimensionality Reduction

High-dimensional data often poses challenges for analysis since relationships between data points can’t be visualized and interpreted directly. To address this, we employ dimensionality reduction techniques. Specifically, we use an autoencoder architecture [5] to project the data into a lower-dimensional space, allowing us to potentially identify decision boundaries. The model consists of two parts: an Encoder $g_{enc}()$ and a Decoder $g_{dec}()$. Each layer in the network is linear with ReLU activation. Batched vectors $R_{in} \in \mathbb{R}^{b \times n}$ - where b is the batch size - are inputted to the model. The dimensionality n decreases layer-wise until it reaches dimension h - dimensionality of encoded vectors $R_{enc} \in \mathbb{R}^h$. In our case, $h = 2$

Fig. 8: Accuracy of model identification classifier under perturbations.


since we want to plot the vectors as points in 2D space. Following that, the decoder increases the dimensionality, outputting reconstructed vector $R_{out} \in \mathbb{R}^n$. To achieve accurately encoded vectors, we need to minimize the Mean Squared Error (MSE) between R_{in} and R_{out} . Due to the inability of reconstruction error to preserve the relations between vectors in the high-dimensional space, we introduce relational loss. This objective preserves the pairwise distances between vectors in the batch after decoding and also in lower-dimensional mapping. Our method adopts a similar framework to Meng *et al.* [33]. Instead of calculating the MSE between Gram matrices, we focus directly on the pairwise l_2 distances between original input vectors and their decoded counterparts, as this preserves the magnitude of the distances and allows us to maintain the original positional relationships in the data. We then calculate the MSE over these pairwise distances, the value of which indicates the average squared error in reconstructing the individual relationships present within the original data. Hence, the objective is the following:

$$\frac{\sum_{i=1}^b \sum_{j=1}^b (\|R_{out}[i,:]\| - \|R_{out}[j,:]\|)^2 - \sum_{i=1}^b \sum_{j=1}^b (\|R_{in}[i,:]\| - \|R_{in}[j,:]\|)^2}{b^2}, \quad (4)$$

where b^2 is the number of pairs of vectors within the batch. Then, the whole objective is as follows:

$$\mathcal{L}_{rdra} = (1 - \alpha) \frac{\sum_{i=1}^b \sum_{j=1}^b (R_{in}[i,j] - R_{out}[i,j])^2}{b^2} + \alpha \frac{\sum_{i=1}^b \sum_{j=1}^b (\|R_{out}[i,:]\| - \|R_{out}[j,:]\|)^2 - \sum_{i=1}^b \sum_{j=1}^b (\|R_{in}[i,:]\| - \|R_{in}[j,:]\|)^2}{b^2} \quad (5)$$

The losses are scaled by hyperparameters $(1 - \alpha)$ and α , where alpha is between 0 and 1. Alpha controls the trade-off between reconstruction accuracy and preservation of pairwise distances. To find the best value, we apply hyperparameter

optimization for each specific set by finding the lowest absolute error and lowest cosine distance for a set of $\alpha \in [0, 1]$.

E Image Generation and Prompt Engineering

All the positive suffixes and negative prompts (presented in Figure 9) are optimized manually by analyzing the quality of the images and how well the generative model follows the instructions. We also provide the list of guiding words for the generative model, which are filled into the original prompts provided in the main work. For painting generation, we use these values:

- **technique** – oil, watercolor, acrylic, digital art, pen and ink;
- **style** – impressionism, abstract, realism, cubism, surrealism, pop art, expressionism, minimalism, post-impressionism, art deco, fauvism, romanticism, baroque, neoclassicism, surreal abstraction, hyperrealism, symbolism, pointillism, suprematism, constructivism, japan art, ukiyo-e, kinetic art, street art, digital art, naïve art, primitivism, abstract expressionism, conceptual art, futurism, precisionism, social realism, magical realism, cubofuturism, lyrical abstraction, tenebrism, synthetic cubism, metaphysical art, graffiti art, videogame art;
- **subject** – landscape, portrait, still life, cityscape, abstract composition, wildlife, fantasy, architecture, seascape, flowers, people, animals, food, music, dance, sports, mythology, history, technology, science, nature, celebrity, space, transportation, underwater, emotion, dreams, folklore, literature;

For face generation, we utilize the following values:

- **age** – baby⁸, young, middle-aged, elderly
- **gender** – male, female
- **hair type** – straight, wavy, curly
- **eyes** – small, large, almond-shaped, round
- **mouth** – thin lips, full lips, wide mouth, narrow mouth
- **expression** – neutral expression, smiling, serious, surprised, angry
- **skin color** – fair, olive, pale, medium, dark
- **glasses** - with glasses, without glasses

All the images are generated with different random seeds for the initial noise to achieve diverse generated content. To remove potential bias, during the image generation, we utilize different schedulers for generation [8] – Euler Discrete, Euler Ancestral [22], DPM-Solver [30], PNDM [28].

⁸ When generating faces of babies, we exclude all the facial characteristics since they are not developed. We prompt the model only with the gender and skin color.

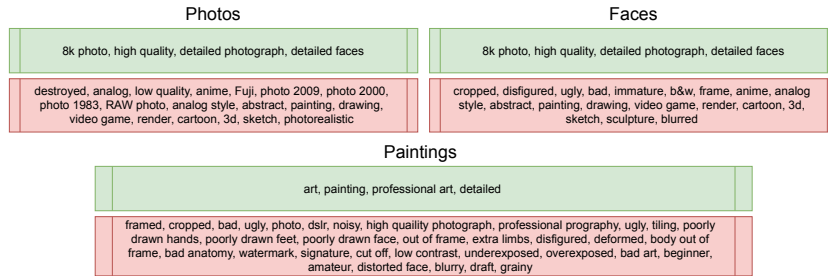


Fig. 9: Positive suffixes (green) and negative prompts (red) utilized for the generation of all generative models requiring prompts.

F Additional Training Details

During the training procedure, the following augmentations are utilized⁹:

1. Pad if needed to 96×96 with reflection borders
2. Random crop 96×96
3. 50% of the images are perturbed by randomly selecting one of the following:
 - JPEG compression with quality $Q \in [50, 95]$
 - WebP compression with quality $Q \in [50, 95]$
 - Gaussian blur with kernel size $k \in [3, 7]$ and standard deviation $\sigma = 0.3 * ((k - 1) * 0.5 - 1) + 0.8$
 - Gaussian noise with variance $\sigma^2 \in [3, 10]$
4. 33% of the images are rotated to 90°
5. 33% of the images are flipped (either horizontally or vertically)

The calibration set consists of an equal number of images from each generator and their real counterparts. During the calibration, we apply the following augmentations:

1. 50% of the images are perturbed:
 - (a) 70% are perturbed by randomly selecting one of the following:
 - JPEG compression with quality $Q \in [50, 95]$
 - WebP compression with quality $Q \in [50, 95]$
 - Gaussian blur with kernel size $k \in [3, 7]$ and standard deviation $\sigma = 0.3 * ((k - 1) * 0.5 - 1) + 0.8$
 - Gaussian noise with variance $\sigma^2 \in [3, 10]$
 - (b) 30% are augmented with all applied in the same order:
 - i. Pad if needed to 256×256 with reflection borders
 - ii. Random resized crop 256×256 , scale $S \in [0.08, 1]$ and ratio $R \in [0.75, 1.33]$
 - iii. 50% are augmented by randomly selecting one of the following:
 - JPEG compression with quality $Q \in [50, 95]$

⁹ No resizing of images is conducted during training.

- WebP compression with quality $Q \in [50, 95]$
- 2. Pad if needed to 256×256 with reflection borders
- 3. Random crop 256×256
- 4. 33% of the images are rotated to 90°
- 5. 33% of the images are flipped (either horizontally or vertically)